EPJ D
Atomic, Molecular, Optical and Plasma Physics
EPJ.org
your physics journal

Eur. Phys. J. D (2014) 68: 220 DOI: 10.1140/epjd/e2014-50165-8

A Multi Water Bag model of drift kinetic electron plasma

Pierre Morel, Florent Dreydemy Ghiro, Vincent Berionni, David Coulette, Nicolas Besse and Özgür D. Gürcan

edp sciences
Società Italiana di Fisica
Springer

Eur. Phys. J. D (2014) 68: 220
DOI: 10.1140/epjd/e2014-50165-8

THE EUROPEAN PHYSICAL JOURNAL D

Regular Article

A Multi Water Bag model of drift kinetic electron plasma*

Pierre Morel[1,2,3,4,a], Florent Dreydemy Ghiro[1,2,3,4], Vincent Berionni[3,2,1,4], David Coulette[5], Nicolas Besse[5], and Özgür D. Gürcan[1,2,3,4]

[1] Université Paris-Sud, UMR 7648, Laboratoire de Physique des Plasmas, 91128 Palaiseau, France
[2] CNRS, UMR 7648, Laboratoire de Physique des Plasmas, 91128 Palaiseau, France
[3] École Polytechnique, UMR 7648, Laboratoire de Physique des Plasmas, 91128 Palaiseau, France
[4] Sorbonne Universités, UPMC Université Paris 06, UMR 7648, Laboratoire de Physique des Plasmas, 91128 Palaiseau, France
[5] Université Lorraine, CNRS, Inst Jean Lamour, UMR 7198, 54506 Vandœuvre Les Nancy, France

Received 28 February 2014 / Received in final form 2 June 2014
Published online 12 August 2014 –

Abstract. A Multi Water Bag model is proposed for describing drift kinetic plasmas in a magnetized cylindrical geometry, relevant for various experimental devices, solar wind modeling... The Multi Water Bag (MWB) model is adapted to the description of a plasma with kinetic electrons as well as an arbitrary number of kinetic ions. This allows to describe the kinetic dynamics of the electrons, making possible the study of electron temperature gradient (ETG) modes, in addition to the effects of non adiabatic electrons on the ion temperature gradient (ITG) modes, that are of prime importance in the magnetized plasmas micro-turbulence [X. Garbet, Y. Idomura, L. Villard, T.H. Watanabe, Nucl. Fusion **50**, 043002 (2010); J.A. Krommes, Ann. Rev. Fluid Mech. **44**, 175 (2012)]. The MWB model is shown to link kinetic and fluid descriptions, depending on the number of bags considered. Linear stability of the ETG modes is presented and compared to the existing results regarding cylindrical ITG modes [P. Morel, E. Gravier, N. Besse, R. Klein, A. Ghizzo, P. Bertrand, W. Garbet, Ph. Ghendrih, V. Grandgirard, Y. Sarazin, Phys. Plasmas **14**, 112109 (2007)].

1 Introduction

A serious difficulty in the modeling of the instabilities and the turbulence in plasmas lies in the large mass ratio between ions and electrons. Consequently, a complete description of a plasma requires a large amount of space and time scales to describe ion and electron dynamics simultaneously, which can make the simulation costs explose [1,2,4]. A widely used hypothesis to circumvent this problem consists in assuming adiabatic electrons, where electron inertia is set to zero due to the smallness of the electron mass. But this approach neglects electron scale physics that can play an important role, for instance by leading to a residual radial heat transport in the case of the micro-turbulence in magnetic fusion plasmas. Taking into account electrons mainly leads to two different types of micro-instabilities in Tokamaks: the electron temperature gradient (ETG) modes and the trapped electron modes (TEM), that take place at space and time scales located in between ion and electron larmor radii and cyclotron frequencies. It should also be noted, that in the non-linear regime, ETG (as well as TEM) induced turbulence is strongly different than the ITG one, since the latter tend to develop Zonal Flows [5,6], that are known to regulate the level of turbulence by predator-prey like behavior [7–9]. On the contrary, ETG and TEM induced turbulence tends to develop radially elongated structures, known as streamers that can be detrimental to plasma confinement [10–19].

In order to describe strongly magnetized plasmas, the Vlasov Maxwell system can be reduced to the gyrokinetic equations, where the fast cyclotron gyration is filtered out so that the gyrokinetic phase space reduces to three space coordinates and the velocity coordinate parallel to the magnetic field, the magnetic moment being an adiabatic invariant [20]. A fundamental property of the Vlasov equation, inherited from Liouville's theorem, and shared with the gyrokinetic Vlasov equation, is that it conserves the phase space volume. Based on this conservation, the Water Bag model consists in choosing a special class of distribution function, taking a multi-step-like form along the parallel velocity coordinate [21–25]. This choice allows to reformulate the gyrokinetic equations into a set of incompressible multi-fluid equations, with an exact closure [26,27].

We consider here the "drift kinetic" limit of the gyrokinetic equations, where the strong magnetic field allows to assume that particles are located on their guiding centers.

* Contribution to the Topical Issue "Theory and Applications of the Vlasov Equation", edited by Francesco Pegoraro, Francesco Califano, Giovanni Manfredi and Philip J. Morrison.

[a] e-mail: pierre.morel@lpp.polytechnique.fr

This allows to suppress finite Larmor radius (FLR) effects, by replacing gyroaverage operator by identity. However the lowest order effect (polarization) can be kept by using an alternative normalization. This model also corresponds to the limit of an infinite aspect ratio tokamak, providing a minimal plasma turbulence model including kinetic effects. Drift kinetic Multi Water Bag model can be used to describe the plasma dynamics in various experimental devices such as magnetized plasma columns [28,29]. Another field of application is the study of space and astrophysical plasma turbulence, for instance in the solar wind [30].

In Section 2, in the general case of kinetic electrons, and with an arbitrary number of kinetic ions, a Multi Water Bag distribution function is introduced for each species, and the general Multi Water Bag model is derived in a cylindrical geometry. In Section 3, by using a standard perturbative method, the linearized Multi Water Bag system is obtained, and the approximation of large radial and azimuthal extents of the linear modes allows to simplify the Laplacian operator. A general form of the Multi Water Bag plasma dielectric function is proposed (Sect. 3.1). In Section 4, the linear stability analysis of a Multi Water Bag electron distribution function with a fixed ion background is then studied in detail, allowing to characterize the Electron Temperature Gradient modes.

2 The Water Bag model for collisionless magnetized plasmas

The fundamental equation describing the evolution of a collisionless plasma is the Vlasov equation:

$$\partial_t f_s(\mathbf{r},\mathbf{v},t) + \dot{\mathbf{r}}.\partial_r f_s(\mathbf{r},\mathbf{v},t) + \dot{\mathbf{v}}.\partial_v f_s(\mathbf{r},\mathbf{v},t) = 0, \quad (1)$$

where $f_s(\mathbf{r},\mathbf{v},t)$ is the distribution function associated with the species s. All the species contribute to the self-consistent electromagnetic fields, given by Maxwell equations:

$$\nabla.\mathbf{E} = \sum_s \frac{q_s}{\epsilon_0}\int f_s(\mathbf{r},\mathbf{v},t)d\mathbf{v}, \quad (2)$$

$$\nabla\times\mathbf{E} = -\frac{\partial\mathbf{B}}{\partial t}, \quad (3)$$

$$\nabla\times\mathbf{B} = \frac{1}{c^2}\frac{\partial\mathbf{E}}{\partial t} + \mu_0\sum_s q_s\int \mathbf{v} f_s(\mathbf{r},\mathbf{v},t)d\mathbf{v}, \quad (4)$$

$$\nabla.\mathbf{B} = 0, \quad (5)$$

and consequently to other species dynamics via the characteristics: $\dot{\mathbf{r}} = \mathbf{v}$, $m_s\dot{\mathbf{v}} = q_s(\mathbf{E}+\mathbf{v}\times\mathbf{B})$. This last remark illustrates the fact that the collisionless character of the Vlasov equation stands for a purely collective interaction between the particles and the waves.

2.1 The Water Bag model

As a consequence of the obvious Hamiltonian structure of the Vlasov equation, the conservation of the phase space volume described by any distribution function f_s is inherited from the Liouville theorem. A special class of distribution function can be chosen, taking the form of a multi-step-like function along the velocity coordinate. The Water Bag model [21–24] and its generalization, the Multi Water Bag model [25–27,31–36], consist in choosing such a class of distribution, where the heights (noted A_j) of the different steps are conserved quantities, as an inheritence of the Liouville theorem. The velocity contours of the Multi Water Bag remain unknown, but are only functions of space and time (noted $v_j^{\pm}(\mathbf{r},t)$), allowing a reduction of one dimension of the problem. In a reduced two dimension phase space x, v_x, the Multi Water Bag distribution function accordingly reads:

$$f^{\mathrm{MWB}}(x,v_x) = \sum_{j=1}^{N} A_j\left[\Upsilon\left(v_x - v_j^+(x,t)\right) - \Upsilon\left(v_x - v_j^+(v,t)\right)\right].$$

This choice is especially suited for cases with only one velocity coordinate, such as gyrokinetic or drift kinetic equations. These equations indeed allow simpler description of magnetized plasmas than the full Vlasov equation, by filtering out the rapid gyromotion of the particles around the magnetic field lines [1,2,20,37–48].

$f_s = f_s(\mathbf{R}, v_\parallel, \mu, t)$ being the guiding-centers distribution function of species s, with $\mathbf{R}$ the guiding-centers coordinates, $v_\parallel$ the velocity coordinate along the magnetic field and μ the magnetic moment (adiabatic invariant), the Gyrokinetic Vlasov equation reads:

$$\partial_t f_s + \dot{\mathbf{R}}.\partial_{\mathbf{R}} f_s + \dot{v_\parallel}\partial_{v_\parallel} f_s = 0, \quad (6)$$

where Gyro-centers characteristics can be written as follows:

$$\dot{\mathbf{R}} = v_\parallel\frac{\mathbf{B}^\star}{B_\parallel^\star} + \mathbf{b}\times\frac{q_s\nabla\langle\phi\rangle_\xi + m_s v_\parallel^2\mathbf{b}.\nabla\mathbf{b} + \mu\nabla B_0}{q_s B_\parallel^\star}, \quad (7)$$

$$\dot{v_\parallel} = -\frac{\mathbf{B}^\star}{B_\parallel^\star}.\frac{\mu\nabla B_0 + q_s\nabla\langle\phi\rangle_\xi}{m_s}, \quad (8)$$

with the modified magnetic field $\mathbf{B}^\star = \mathbf{B}_0 + \frac{m_s v_\parallel}{q_s}\nabla\times\mathbf{b}$, $\mathbf{b}$ the unit vector along the magnetic field: $\mathbf{b} = \mathbf{B}_0/B_0$, and $B_\parallel^\star = \mathbf{b}.\mathbf{B}^\star$. In gyrokinetic theory, the gyroaverage of the electrostatic potential $\langle\phi\rangle_\xi$ is required to take into account the contributions of the real particles located on a Larmor radius distance $\mathbf{r} = \mathbf{R}+\rho_{\mathcal{L}}$ around a given guiding center $\mathbf{R}$.

In the electrostatic case, the system is closed with the Poisson equation, written for the electrostatic potential:

$$-\nabla^2\phi - \sum_s \nabla_\perp.\frac{\omega_{ps}^2\nabla_\perp\phi}{\Omega_{cs}^2} = \sum_s\frac{q_s}{\epsilon_0}\int\langle f_s\rangle_\xi\mathcal{J}_s d\mu dv_\parallel, \quad (9)$$

where the gyroaverage of the guiding-centers distribution function $\langle f_s\rangle_\xi$ allows to sum contribution of a ring of guiding centers.

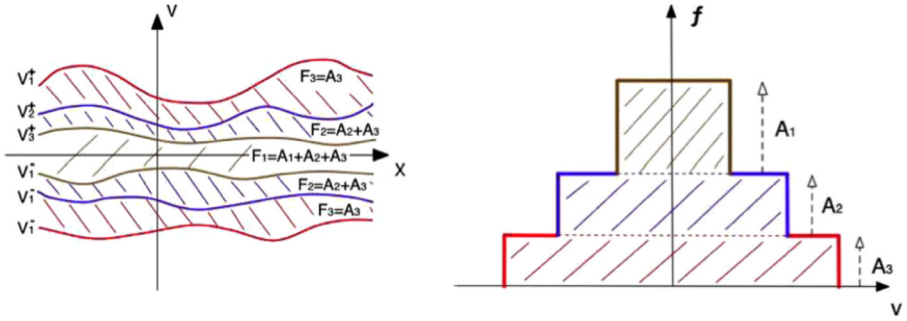

Fig. 1. Multi Water Bag distribution function in (x, v) plane (left) and step-like dependence along velocity coordinate (right).

It is evident from equation (6), that the gyrokinetic Vlasov equation only admits the parallel velocity variable $v_\parallel$ as an independent coordinate. This result allow the use of a Multi Water Bag distribution function: the adaptation of such a model in a gyrokinetic framework including finite Larmor radius effects and magnetic inhomogeneities has been described in previous works [26,27], focusing on the physics of kinetic ions with adiabatic electrons.

However, our aim here is to focus on the description of an arbitrary number of kinetic species, and the simplest description retaining kinetic effects for such a problem is the drift kinetic equation in a cylindrical geometry. In this limit finite Larmor radius effects related to gyrokinetic averaging are neglected.

The assumption of a cylindrical geometry with a homogeneous magnetic field allows to neglect curvature and gradient of the magnetic field as well, the resulting reduced model reads:

$$\partial_t f_{s\mu} + \frac{\mathbf{b}\times\nabla\phi}{B_0}.\nabla_\perp f_{s\mu} + v_\parallel \nabla_\parallel f_{s\mu} - \frac{q_s \nabla_\parallel \phi}{m_s}\partial_{v_\parallel} f_{s\mu} = 0, \tag{10}$$

$$-\nabla^2\phi = \sum_s \frac{q_s}{\epsilon_0}\sum_\mu \int f_{s\mu} dv_\parallel, \tag{11}$$

for an arbitrary number of species s. Since we neglect finite Larmor radius effects, there is no dependence on the magnetic moment μ in the resulting equations. μ indices and summation along μ will also be removed in the following.

At this point it is important to notice that when electron dynamics is considered, the Laplacian operator in the Poisson equation can not be neglected, since the electron gyro radius can be the same order of magnitude as the electron Debye length: $\epsilon_L = \lambda_{De}^2/\rho_e^2 = \Omega_{ce}^2/\omega_{pe}^2 \approx 10^{19} B_0^2/n_{e0}$[1]. This results in a major difference with ITG linear analysis, where finite Larmor radius effects are important since they introduce via the polarization term a perpendicular Laplacian in the quasi-neutrality equation, while the ETG linear physics already contains a Laplacian due to the necessity of using Poisson equation. It results that finite Larmor radius effects does not introduce fundamentally new physics regarding linear ETG modes and can be neglected in the following.

For each species s to be considered, we make the choice of a Multi Water Bag distribution function along the parallel velocity coordinate:

$$f_s(\mathbf{r}, v_\parallel, t) = \sum_{j=1}^{N_s} A_{sj}\left[\Upsilon\left(v_\parallel - v_{sj}^-(\mathbf{r},t)\right) - \Upsilon\left(v_\parallel - v_{sj}^+(\mathbf{r},t)\right)\right], \tag{12}$$

with $x \mapsto \Upsilon(x)$ the Heaviside step function. Each bag j is defined by the discontinuity A_{sj} and the two velocity contours $v_{sj}^\pm(\mathbf{r}, t)$. The value of each discontinuity A_{sj} remains constant as long as binary interactions (collisions) can be neglected: this major property is a consequence of Liouville's theorem, constraining the distribution function to be constant along its characteristics. For each species s, an arbitrary number of bags N_s can be used, which is kept small, typically few tenth, for convenience. An illustration of the Multi Water Bag distribution function is given in Figure 1.

By inserting the Multi Water Bag distribution function (12) into the drift kinetic Vlasov equation (10), we obtain for each bag a couple of equations governing the dynamics of the velocity contours $v_{sj}^\pm(\mathbf{r}, t)$:

$$\partial_t v_{sj}^\pm + \mathbf{v}_E.\nabla_\perp v_{sj}^\pm + v_{sj}^\pm \nabla_\parallel v_{sj}^\pm = -\frac{q_s\nabla_\parallel\phi}{m_s}, \tag{13}$$

where the partial derivative of the distribution function along the parallel velocity is replaced by a source of acceleration by the parallel electric field.

All contours are coupled by the Poisson equation, where the continuous integration along the parallel velocity coordinate is replaced by a discrete sum along the bags:

$$-\nabla^2\phi = \sum_s \frac{q_s}{\epsilon_0}\sum_{j=1}^{N_s} A_{sj}\left[v_{sj}^+ - v_{sj}^-\right]. \tag{14}$$

2.2 Momentum sense equivalence

As pointed out by Gros et al. [49], an important property of the Multi Water Bag model is that it gives a connection between Vlasov and hydrodynamic descriptions.

[1] $\epsilon_L \approx 10$ for a typical cylindrical plasma column ($B_0 \approx 80$ mT, $n_{e0} \approx 5\times10^{15}$ m^{-3}), $\epsilon_L \approx 2$ for a typical Tore Supra plasma ($B_0 \approx 3$ T and $n_{e0} \approx 4\times10^{19}$ m^{-3}).

It is indeed possible to rewrite the couples of Multi Water Bag contours equations (13), as a set of continuity and Euler equation for each bag j, by defining a bag density $n_{sj} = A_{sj}\left[v_{sj}^{+} - v_{sj}^{-}\right]$ and a bag mean velocity $u_{sj} = \left[v_{sj}^{+} + v_{sj}^{-}\right]/2$. We obtain:

$$\partial_t n_{sj} + \nabla_\perp.\left(\mathbf{v}_E n_{sj}\right) + \nabla_\parallel\left(n_{sj}u_{sj}\right) = 0, \tag{15}$$

$$\partial_t u_{sj} + \mathbf{v}_E.\nabla_\perp u_{sj} + u_{sj}\nabla_\parallel u_{sj} = -\frac{\nabla_\parallel P_{sj}}{m_s n_{sj}} - \frac{q_s\nabla_\parallel\phi}{m_s}, \tag{16}$$

where the expression of the partial pressure of the jth bag can be obtained without any other assumption: $P_{sj} = m_j n_{sj}^3/(12A_{sj})$.

Going further with the correspondence between the Multi Water Bag and any continuous distribution function, the successive moments of the Multi Water Bag can be defined:

$$\mathcal{M}_{\ell,s}^{\mathrm{MWB}} = \sum_{j=1}^{N_s}\alpha_{sj}a_{sj}^{\ell}, \tag{17}$$

where an equilibrium has been defined, with density n_{s0} for species s, symetric contours: $\left(v_{sj}^{\pm}\right)^0 = \pm a_{sj}$, and the normalized bag density has been introduced: $\alpha_{sj} = 2A_{sj}a_{sj}/n_{s0}$.

The Multi Water Bag equilibrium parameters A_{sj} and a_{sj} being at this point entirely free, we have to use physical constraints to compare the Multi Water Bag equilibrium to a given reference distribution function:

$$f_{s0} = f_{s0}\left(n_{s0}, T_{s0}, \frac{m_s v_\parallel^2}{T_{s0}}\right). \tag{18}$$

In the considered case of cylindrical geometry, the equilibrium is assumed to depend only on the radial coordinate. In the reference continuous distribution function (18), this dependence is contained in the density and temperature profiles $n_{s0}(r)$ and $T_{s0}(r)$.

A method allowing to fix the Multi Water Bag free parameters consists in the momentum sense equivalence: the MWB moments and their radial gradients are identified to the corresponding continuous distribution function moments $\mathcal{M}_{s\ell}(f_{s0}) = \int_{-\infty}^{+\infty} v_\parallel^\ell f_{s0}dv_\parallel$, up to an order fixed by the number of bags N_s chosen [50]. We then obtain a Vandermonde system:

$$\mathbf{V}_{sj\ell}\alpha_{sj} = (\ell+1)\,\mathcal{M}_{s\ell}, \tag{19}$$

$$\mathbf{V}_{sj\ell}\beta_{sj} = \ell\mathcal{M}_{s\ell}, \tag{20}$$

$$\mathbf{V}_{sj\ell}\gamma_{sj} = \mathcal{M}_{s\ell}, \tag{21}$$

with the Vandermonde matrix: $\mathbf{V}_{sj\ell} \equiv a_{sj}^{\ell}$, where the equilibrium bag contours a_{sj} are given, and the unknowns are the parameters α_{sj}, β_{sj} and γ_{sj}, defined so that the Multi Water Bag equilibrium radial gradients:

$$\kappa_{sj} = d_r\ln a_{sj} \tag{22}$$

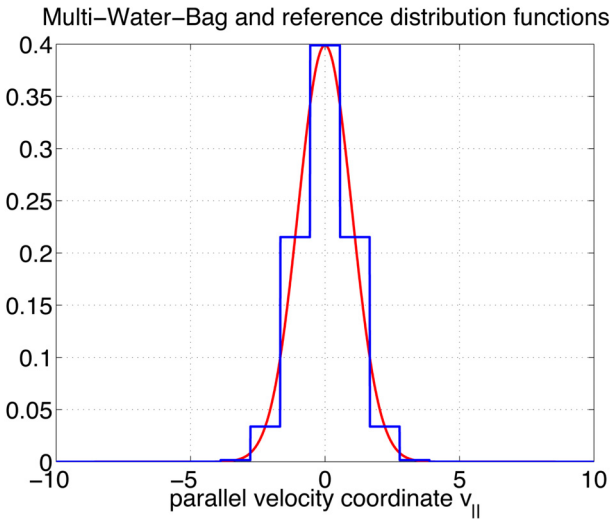

Fig. 2. Comparison between the Multi Water Bag distribution function and a reference continuous one (Maxwellian), as functions of the parallel velocity $v_\parallel$.

are a linear combination of the ones prescribed by the density ($\kappa_{ns} = d_r\ln n_{s0}$) and temperature profiles ($\kappa_{Ts} = d_r\ln T_{s0}$):

$$\alpha_{sj}\kappa_{sj} \equiv \frac{\beta_{sj}}{2}\kappa_{Ts} + \gamma_{sj}\kappa_{ns}. \tag{23}$$

The inversion of a Vandermonde system can be done analytically for a moderate number of bags, typically lower than 10. Beyond this value, the inverse matrix coefficients become numerically unstable, and an approximate method is chosen [50]. An illustration of the Multi Water Bag distribution function superimposed with a reference Maxwellian distribution function is given in Figure 2, where the Multi Water Bag parameters have been obtained by inverting the Vandermonde system (19)−(21).

3 Linear stability of drift kinetic electron plasma

In this section, we focus on the problem of the linear stability of a kinetic electron population. As a first step, we derive the expression of the plasma dielectric function with a Multi Water Bag representation, in the general case of an arbitrary number of ion species. We then examine the case of Multi Water Bag kinetic electrons with adiabatic ion response, in order to study the linear stability properties of the cylindrical branch of electron temperature gradient (ETG) modes.

3.1 The Multi Water Bag dielectric plasma function

Linearization of the cylindrical Multi Water Bag, drift kinetic equations can be achieved by choosing a stationary equilibrium depending only on the radial coordinate, without any equilibrium electrostatic potential, and considering small perturbations, expressed in a Fourier basis for

the time, poloidal and azimuthal coordinates:

$$v_{sj}^{\pm}(r,\theta,z,t) = \pm a_{sj}(r) + \widetilde{\delta v}_{sj}^{\pm}(r) e^{i\left(m\theta + k_{\parallel} z - \omega t\right)}, \quad (24)$$

$$\phi(r,\theta,z,t) = 0 + \widetilde{\delta\phi}(r) e^{i\left(m\theta + k_{\parallel} z - \omega t\right)}. \quad (25)$$

Inserting these expressions into the nonlinear Multi Water Bag equations, we obtain, at zeroth order in perturbation, a characterization of the equilibrium:

$$a_{sj} \nabla_{\parallel} a_{sj} = 0, \quad (26)$$

$$\sum_s q_s \sum_j 2 A_{sj} a_{sj} = 0, \quad (27)$$

where the second equation is nothing but the Multi Water Bag version of the quasi-neutrality condition.

At first order in perturbation, we obtain:

$$\widetilde{\delta v}_{sj}^{\pm} = \frac{q_s}{m_s} \frac{k_{\parallel} \mp k_\theta d_r a_{sj}/\Omega_{cs}}{\omega \mp k_{\parallel} a_{sj}} \widetilde{\delta\phi}, \quad (28)$$

$$-\triangle\phi = \sum_s \frac{q_s}{\epsilon_0} \sum_j A_{sj} \left(\widetilde{\delta v}_{sj}^{+} - \widetilde{\delta v}_{sj}^{-} \right), \quad (29)$$

where the poloidal wave vector $k_\theta \equiv m/r$ as well as the cyclotron pulsations $\Omega_{cs} \equiv q_s B_0/m_s$ appear.

Finally, by substituting velocities of the perturbed contours (28) into the perturbed Poisson equation (29), we obtain the Multi Water Bag dispersion relation:

$$\triangle\phi + \left\{ \sum_s \omega_{ps}^2 \sum_j \alpha_{sj} \frac{k_{\parallel}^2 - \omega k_\theta \kappa_{sj}/\Omega_{cs}}{\omega^2 - k_{\parallel}^2 a_{sj}^2} \right\} \phi = 0, \quad (30)$$

where $\omega_{ps}^2 \equiv q_s^2 n_{s0}/(\epsilon_0 m_s)$ is the plasma pulsation for each species s.

At this point, the presence of the Laplacian operator left us with a second order differential equation. We can however simplify this strongly by assuming that radial and azimuthal eigenmodes are very elongated compared to the Debye length. Such an assumption is motivated by the fact that ETG modes are known to lead to the formation of streamers. By writting schematically the cylindrical Laplacian as a sum of some squared wave vectors k_r, k_θ and $k_{\parallel}$, this leads to the assumption:

$$\lambda_{De}^2 \triangle\phi \sim -\left[\lambda_{De}^2 k_r^2 + \lambda_{De}^2 k_\theta^2 + \lambda_{De}^2 k_{\parallel}^2 \right] \phi \approx -\lambda_{De}^2 k_\theta^2 \phi,$$

where $k_\theta = m/r$.

Since the aim of this work is to describe ETG stability, we choose the following normalizations:

$$\begin{aligned} \widehat{a}_{sj} &= a_{sj}/v_{Ts}, \\ \widehat{k_{\parallel}} &= k_{\parallel} R_0, \\ \widehat{\omega} &= \omega R_0/v_{Te}, \\ \widehat{k_\theta} &= k_\theta v_{Te}/\left|\Omega_{ce}\right|, \\ \widehat{\kappa_{sj}} &= R_0 \kappa_{sj}, \end{aligned} \quad (31)$$

where $v_{Ts}^2 \equiv T_{s0}/m_s$ is the thermal velocity, R_0 is the radius of the cylinder assumed to be the same order as the characteristic parallel length scale, and $\Omega_{ce} = q_e B_0/m_e$ is the (negative) electron cyclotron pulsation.

For simplicity, the polarization term in the gyrokinetic Poisson equation (9) has been neglected, along with finite Larmor radius effects. However taking this effect into account will not modifiy the results qualitatively, since by using an alternative normalization:

$$\widehat{k_\theta}' = \sqrt{1 + \sum_s \frac{\omega_{ps}^2}{\Omega_{cs}^2}} \widehat{k_\theta} \quad (32)$$

$$\widehat{\kappa_{sj}}' = \frac{1}{\sqrt{1 + \sum_s \omega_{ps}^2/\Omega_{cs}^2}} \widehat{\kappa_{sj}}, \quad (33)$$

calculations presented in the following remain unchanged. The aforementionned normalization can be recovered by replacing the Laplacian in the left hand side of equation (29) by the sum of the Laplacian and the polarization term, where we neglect the radial variations of the electrostatic potential. We then obtain the expression:

$$-\triangle\phi - \nabla_\perp \left(\sum_s \frac{\omega_{ps}^2}{\Omega_{cs}^2} \nabla_\perp \phi \right) \approx \left(1 + \sum_s \frac{\omega_{ps}^2}{\Omega_{cs}^2} \right) k_\theta^2 \phi, \quad (34)$$

where the new choice of normalization for k_θ becomes evident.

Using the aforementioned approximation for the Laplacian of the electrostatic potential, the normalized plasma dispersion relation can be written as follows:

$$\epsilon(\omega, k_\theta, k_{\parallel}) \cdot \widetilde{\delta\phi} = 0, \quad (35)$$

where we have defined the Multi Water Bag dielectric plasma function:

$$\epsilon(\omega, k_\theta, k_{\parallel}) = \frac{\Omega_{ce}^2 k_\theta^2}{\omega_{pe}^2} - \sum_s \frac{Z_s n_{s0}}{n_{e0}} \sum_j \alpha_{sj} \frac{Z_s \sigma_s k_{\parallel}^2 - \omega k_\theta \kappa_{sj}}{\omega^2 - \sigma_s \tau_s k_{\parallel}^2 a_{sj}^2}, \quad (36)$$

where we have introduced the mass $\sigma_s = m_e/m_s$, charge $Z_s = q_s/|q_e|$, and temperature $\tau_s = T_{s0}/T_{e0}$ ratios.

Focusing on the electron response ($\sigma_s = 1$, $Z_s = -1$ and $\tau_s = 1$), the dispersion equation reads:

$$\frac{\Omega_{ce}^2}{\omega_{pe}^2} k_\theta^2 + \mathcal{R}_i - \sum_j \alpha_{je} \frac{k_{\parallel}^2 + \omega k_\theta \kappa_{je}}{\omega^2 - k_{\parallel}^2 a_{je}^2} = 0, \quad (37)$$

where $\mathcal{R}_i$ symbolizes the ion response, on which approximations can be made:

– the case of a single ion bag gives the ion response:

$$\mathcal{R}_i = \left(k_\theta \kappa_{ni} \omega - Z_i \mu_i k_{\parallel}^2 \right) / \left(\omega^2 - \mu_i \tau_i k_{\parallel}^2 \right);$$

– considering cold ions $T_{i0} = 0$ leads to:

$$\mathcal{R}_i = \left(k_\theta \kappa_{ni} \omega - Z_i \mu_i k_{\parallel}^2 \right) / \omega^2;$$

– heavy ion limit can be considered $\sigma_s \longrightarrow 0$, and the associated ion response becomes:

$$\mathcal{R}_i = k_\theta \kappa_{ni}/\omega;$$

– adiabatic ions limit is usual in a magnetic fusion study of ETG modes:

$$\mathcal{R}_i = Z_i \frac{T_i}{T_e}.$$

In order to study pure ETG stability, we consider in the following the latest limit of adiabatic Hydrogen isotopes ions, with $Z_i = 1$ and $T_i = T_e$, the dispersion equation reduces to:

$$1 + \frac{\Omega_{ce}^2}{\omega_{pe}^2} k_\theta^2 - \sum_j \alpha_{je} \frac{k_\parallel^2 + \omega k_\theta \kappa_{je}}{\omega^2 - k_\parallel^2 a_{je}^2} = 0. \tag{38}$$

3.2 Linear Multi Water Bag stability threshold

For an arbitray number of bags N_s, there is no general expression for the stable and unstable roots of the dielectric plasma function (38). However, a general criterion for the stability frontier can be formulated as follows:

$$\begin{aligned} \epsilon(\omega, k_\theta, k_\parallel) &= 0, \\ \partial_\omega \epsilon(\omega, k_\theta, k_\parallel) &= 0. \end{aligned} \tag{39}$$

By using the assumed link (23) between the MWB parameters (β_{je} and γ_{je}) on one side, and the equilibrium density (κ_{ne}) and temperature (κ_{Te}) profiles on the other side, we can rewrite the dielectric plasma function as follows:

$$\begin{aligned} \epsilon(\omega, k_\theta, k_\parallel) = \left(1 + \frac{\Omega_{ce}^2}{\omega_{pe}^2} k_\theta^2\right) - \sum_j \frac{k_\parallel^2 \alpha_{je}}{\omega^2 - k_\parallel^2 a_{je}^2} \\ - \sum_j \frac{\omega k_\theta \beta_{je}}{\omega^2 - k_\parallel^2 a_{je}^2} \kappa_{ne} - \frac{\omega k_\theta \gamma_{je}}{\omega^2 - k_\parallel^2 a_{je}^2} \frac{\kappa_{Te}}{2}. \end{aligned} \tag{40}$$

The marginal stability system (39) can be interpreted as a system of unknowns κ_{ne}, κ_{Te} defining the stability frontier, parametrized by ω, for a fixed couple $(k_\theta, k_\parallel)$. It is then possible to solve numerically this system and to obtain a Multi Water Bag stability threshold for ETG modes.

In Figure 3, the linear stability threshold obtained by solving the system (39) parametrized by ω is given in the plane of density and temperature logarithmic gradients $(\kappa_{ne}, \kappa_{Te})$. Parameters used are as simple as possible: $N_e = 20$ bags, $a_{N_e} = 6v_{Te}$, $k_\theta = 1$, $k_\parallel = 1$ and $\Omega_{ce} = \omega_{pe}$. Superimposed is the analytical result obtained with a Maxwellian distribution function, according to references [27,51]:

$$\kappa_{Te}^{\pm} = \kappa_{ne} \pm \sqrt{\kappa_{ne}^2 + 4 \frac{X(X+1)k_\parallel^2}{k_\theta^2}}, \tag{41}$$

where $X = 1 + \Omega_{ce}^2 k_\theta^2 / \omega_{pe}^2$.

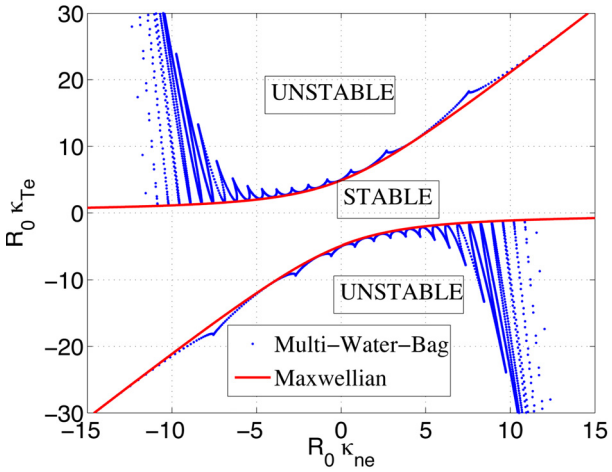

Fig. 3. Illustration of the MWB linear stability threshold obtained with a MWB model for Electron Temperature Gradient instability, in the plane of the electron density and temperature gradients (κ_{ne} and κ_{Te}). $N_e = 20$ bags, $a_{N_e} = 6v_{Te}$, $k_\theta = 1$, $k_\parallel = 1$ and $\Omega_{ce} = \omega_{pe}$.

The overall agreement between the Multi Water Bag and Maxwellian linear stability threshold is excellent, with discrepancies due to the discrete nature of the MWB description: the lobe-like structure of the MWB linear stability threshold has indeed already been observed in previous studies [3]. In the same reference, authors have found that for $N = 10$ bags and $a_{\max} = 5v_{Ti}$, the linear growth rate reaches 98.5% of the value obtained in the continuous limit $N \longrightarrow \infty$, so that we can consider that for the values $N_e = 20$ bags and $a_{\max} = 6v_{Te}$ chosen here, the results can be interpreted with good confidence.

The unstable domain is characterized by a slope $\eta_e = \kappa_{Te}/\kappa_{ne} \longrightarrow 2$ for the large values of the logarithmic gradients κ_{ne}, κ_{Te}: this is a known result in the case of cylindrical temperature gradient modes [3,51]. In the regions close to the center, the stability frontier departs from this slope and tends to zero in the second and fourth quadrants of the stability diagram. This is also the region where the MWB and maxwellian thresholds differ significantly but this region, corresponding to opposite peaking of density and temperature profiles, is physically irrelevant.

4 A Multi Water Bag analysis of cylindrical ETG modes

In this section, the linear properties of the cylindrical Electron Temperature Gradient modes are studied into details:

– analytical results concerning the linear growth rate and pulsation of ETG are derived in the limit of pulsations far from resonances $\omega \gg k_\parallel a_{je}$, corresponding to a fluid model;
– the dependence of the linear growth rate and the associated pulsation on the electron density and temperature gradients is analyzed first;
– the spectral repartition of the unstable modes is studied in the plane of poloidal and azimuthal wave vectors.

4.1 Fluid limit

The limit $k_\parallel v_{Te}/\omega \longrightarrow 0$ corresponds to considering a plasma far from the resonances $\omega \simeq k_\parallel a_{je}$, i.e. a fluid limit. In this limit, the MWB dielectric plasma function can be simplified, using the approximation:

$$\frac{1}{\omega^2 - k_\parallel^2 a_{je}^2} \approx \frac{1}{\omega^2}\left[1 + \frac{k_\parallel^2 a_{je}^2}{\omega^2} + \mathcal{O}\left(\frac{k_\parallel^4 a_{je}^4}{\omega^4}\right)\right], \quad (42)$$

we obtain the following fourth order polynomial as an approximation of the dielectric plasma function:

$$\begin{aligned}\epsilon(\omega, k_\theta, k_\parallel) \simeq \left(1 + \frac{\Omega_{ce}^2 k_\theta^2}{\omega_{pe}^2}\right)\omega^4 - k_\theta \sum_j \alpha_{je}\kappa_{je}\omega^3 \\ - k_\parallel^2 \sum_j \alpha_{je}\omega^2 - k_\parallel^2 k_\theta \sum_j \alpha_{je} a_{je}^2 \kappa_{je}\omega \\ - k_\parallel^4 \sum_j \alpha_{je} a_{je}^2.\end{aligned}$$

For consistency purpose with (42), we have to neglect the last term in the previous equation, since it is fourth order in $k_\parallel/\omega$. By using the momentum sense equivalence, we get:

$$\begin{aligned}\epsilon(\omega, k_\theta, k_\parallel) \simeq \left(1 + \frac{\Omega_{ce}^2 k_\theta^2}{\omega_{pe}^2}\right)\omega^4 - k_\theta \kappa_{ne}\omega^3 - k_\parallel^2 \omega^2 \\ - k_\parallel^2 k_\theta \left(\kappa_{ne} + \kappa_{Te}\right)\omega. \quad (43)\end{aligned}$$

The stability condition for a third order polynomial can be expressed, as well as the expression of the complex roots if they exist. The detailed expression of the linear stability threshold in the fluid limit reads:

$$\begin{aligned}\kappa_{Te}^{\pm} = \frac{2k_\theta^4\kappa_{ne}^3 k_\parallel^2 + 9\xi\left(1+3\xi\right)k_\theta^2\kappa_{ne}k_\parallel^4}{27\xi^2 k_\theta^2 k_\parallel^4} \ldots \\ \pm 4\frac{\sqrt{27\xi^3 k_\theta^2 k_\parallel^{10} - 27\xi^2 k_\theta^4\kappa_{ne}^2 k_\parallel^8 + 9\xi k_\theta^6\kappa_{ne}^4 k_\parallel^6 - 2k_\theta^8\kappa_{ne}^6 k_\parallel^4}}{27\xi^2 k_\theta^2 k_\parallel^4}, \quad (44)\end{aligned}$$

where we used the definition: $\xi = 1 + k_\theta^2\Omega_{ce}^2/\omega_{pe}^2$.

In the unstable domain, the expression of the linear growth rate and the associated pulsation take the complicated following forms:

$$\gamma = \frac{\sqrt{3}}{2}\left|\sqrt[3]{\frac{-q}{2} + \sqrt{\frac{q^2}{4} + \frac{p^3}{27}}} - \sqrt[3]{\frac{-q}{2} - \sqrt{\frac{q^2}{4} + \frac{p^3}{27}}}\right|, \quad (45)$$

$$\omega = -\frac{1}{2}\left[\sqrt[3]{\frac{-q}{2} + \sqrt{\frac{q^2}{4} + \frac{p^3}{27}}} + \sqrt[3]{\frac{-q}{2} - \sqrt{\frac{q^2}{4} + \frac{p^3}{27}}}\right], \quad (46)$$

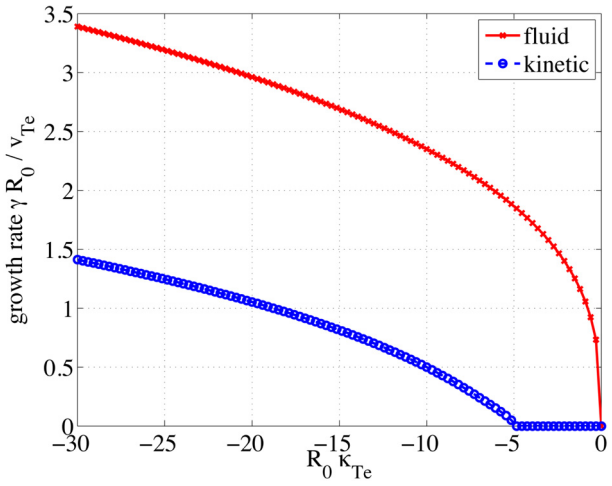

Fig. 4. Linear growth rate γ as a function of the logarithmic density gradient κ_{Te} for a flat density profile $\kappa_{ne} = 0$, as computed from the complete MWB dispersion relation (38), or as given in the fluid limit (49).

where we used the notations:

$$q = -\frac{2k_\theta^3\kappa_{ne}^3 + 9\xi k_\theta\kappa_{ne}k_\parallel^2 + 27\xi^2 k_\theta(\kappa_{ne}+\kappa_{Te})k_\parallel^2}{27\xi^3}, \quad (47)$$

$$p = \frac{k_\theta^2\kappa_{ne}^2 - 3\xi k_\parallel^2}{3\xi^2}. \quad (48)$$

In the special case of a flat density profile, $\kappa_{ne} = 0$, a simple expression can be obtained for the linear growth rate:

$$\gamma \simeq \frac{\sqrt{3}}{2}\sqrt[3]{\frac{k_\parallel^2 k_\theta\left|\kappa_{Te}\right|}{2\xi}}, \quad (49)$$

with this formula, a comparison is possible with the values obtained by solving the complete dispersion relation, i.e. taking into account resonances. The result is given in Figure 4, where the growth rates are compared in the case of a flat density profile. It is clear that the fluid limit overestimates, approximately doubles, the growth rate, and we recover a known issue that fluid models fail to capture correctly even the linear physics, whenever kinetic effects such as resonances are important.

4.2 Linear stability in the plane of electron density and temperature gradients

By solving the roots of the dielectric MWB plasma function (38), we have an access to the linear growth rate and the associated frequency in the unstable domain given in Figure 3.

In Figure 5, the normalized growth rate $\gamma R_0/v_{Te}$ and in Figure 6 the associated frequency $\omega R_0 v_{Te}$ are given as functions of the normalized electron density $R_0\kappa_{ne}$ and temperature $R_0\kappa_{Te}$ gradients, corresponding to a zoom of the linear stability threshold given previously (Fig. 3).

It can be observed in Figure 5 that the marginal stability threshold coincides with the values of the linear growth

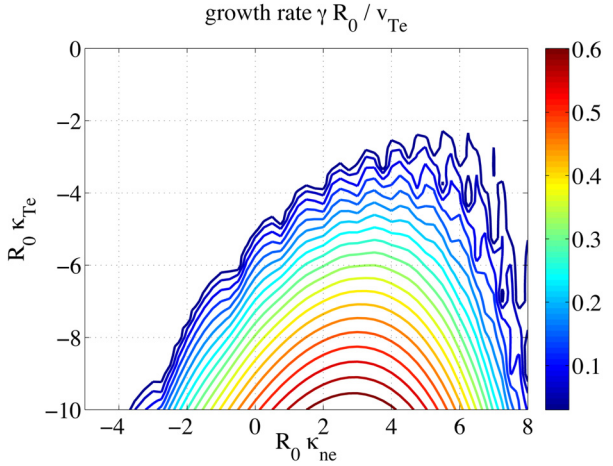

Fig. 5. Linear growth rate γ as a function of the electron density and temperature gradients (κ_{ne} and κ_{Te}). Parameters are those of Figure 3.

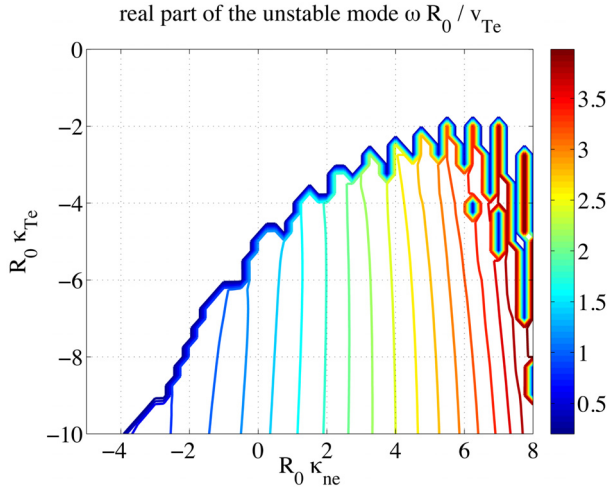

Fig. 6. Pulsation of the unstable mode ω, as a function of the electron density and temperature gradients (κ_{ne} and κ_{Te}). Parameters are those of Figure 3.

rate γ. The typical MWB lobe-like structure of the stability threshold penetrates moderately into the unstable region and also affects the vicinity of the stability frontier. A global increase of the linear growth rate is observed as increasing the distance from the linear stability threshold.

In Figure 6, the repartition of the values of the pulsations associated to the unstable ETG mode is totally different than the trend observed for the associated growth rates: a structure of roughly vertical bands of iso-pulsation contours can be observed.

This allows to illustrate the fact that the pulsations of the unstable modes are associated to increasing phase velocities, roughly proportional to the normalized density gradient, and without a strong dependence on the normalized temperature gradient. The link with the Multi Water Bag description and the associated equilibrium velocities $\pm a_{je}$ and parallel resonances $\pm k_{\|} a_{je}$ makes clear the fact that the ETG modes are excited from the very core of the distribution function, associated to the fluid limit, for the large negative values of the density gradients, up to the tail of the distribution function, associated to kinetic effects, by increasing the value of the density gradient.

4.3 Linear stability in the plane of the poloidal and parallel wave vectors

An important property of the dielectric plasma function (38) derived for the study of ETG modes, lies in the remniscence of the Laplacian operator, that introduces a poloidal mode selection (term $\propto \lambda_{De}^2 k_\theta^2$). In the case of ITG modes in cylindrical geometry, if the polarization effect are neglected, the linear properties would have been in turn scale invariant with respect to k_θ, that is just acting as a prefactor in the characteristic length of the logarithmic gradients $\widetilde{\kappa_{je}} = k_\theta \kappa_{je}$. This is the main reason why the polarization term plays a more important role for ITG linear physics.

In the present case, the plasma dielectric function can be strongly affected by a change of the value of the poloidal wave vector k_θ, since it not only appear as a prefactor of the gradients, but also in the constant term inherited from the Laplacian.

On the other hand, the dielectric plasma function is left invariant by rescaling the parallel wave vector: this property can be illustrated by considering the new variables: $\widetilde{\omega} = \omega/k_{\|}$ and $\widetilde{\kappa}_{je} = \kappa_{je}/k_{\|}$. Under this change of variables, it appears clearly that the plasma dielectric function:

$$\epsilon(\widetilde{\omega}, k_\theta) = 1 + \frac{k_\theta^2 \Omega_{ce}^2}{\omega_{pe}^2} - \sum_j \alpha_{je} \frac{1 + k_\theta \widetilde{\kappa}_{je} \widetilde{\omega}}{\widetilde{\omega}^2 - a_{je}^2}, \qquad (50)$$

will not be affected by a change in $k_{\|}$, and that the only changes will concern the frequencies ω as well as the gradients κ_{je} in order to keep $\widetilde{\omega}$ and $\widetilde{\kappa}_{je}$ constant.

In Figure 7, the linear growth rate γ has been computed as a function of the normalized poloidal and azimuthal wave vectors $(k_\theta v_{Te}/\Omega_{ce}, R_0 k_{\|})$, for three couples of the logarithmic density and temperature profiles $(\kappa_{ne}, \kappa_{ne})$, corresponding to the fluid branch close to linear stability threshold ($R_0\kappa_{ne} = -10$, $R_0\kappa_{Te} = -25$), to the kinetic branch close to marginal stability ($R_0\kappa_{ne} = 0$, $R_0\kappa_{Te} = -10$), and to a case in the core of the unstable domain ($R_0\kappa_{ne} = 0$, $R_0\kappa_{Te} = -25$).

The spectral location of the maximum growth rate is not affected by the distance to the threshold, or the type of branch considered, and the peak remains approximately located around ($k_\theta v_{Te}/\omega_{ce} \approx 1$, $R_0 k_{\|} \approx 1$).

On the contrary, the values of the maximum growth rate, are strongly affected by the distance to the threshold. As well, the spectral extension of the unstable region increases with the distance to the threshold.

To conclude this section, the main result concerning the dependence of the ETG instability on the parallel and poloidal wave vectors, lies in the fact that the ETG modes present a finite poloidal extent, while their radial extent

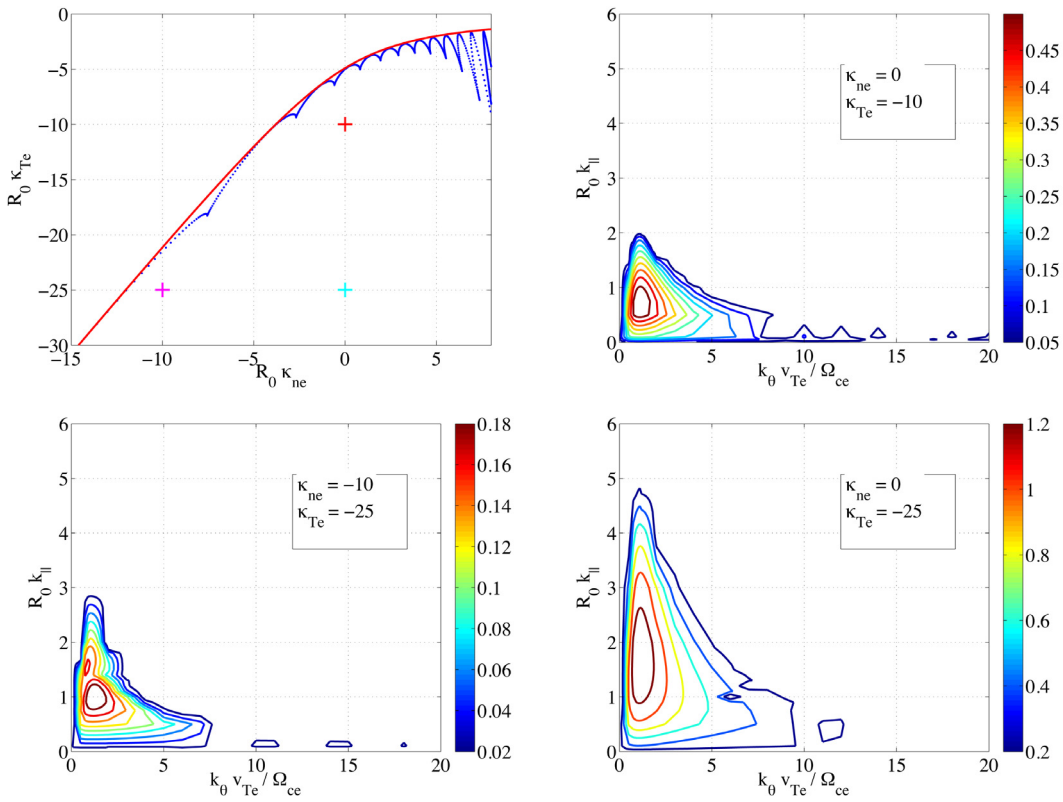

Fig. 7. Linear growth rate γ as a function of the parallel and poloidal wave-vectors (resp. $k_{\parallel}$ and k_{θ}), for three different points in the $(\kappa_{ne}, \kappa_{Te})$ plane.

is assumed be much larger, leading to streamer structures [16,17]. ETG linear stability presented here shows a mode structure very similar to ITG modes, the main difference being that the ion length scales allow to neglect the Laplacian operator in Poisson equation and also makes very important to include finite Larmor radius effects. Without FLR effects, the ITG linear stability leads to very different results, since by neglecting the Poisson Laplacian, there is no mechanism for a selection of a most unstable growth rate along k_{θ} [3]. On the contrary, by taking into account finite Larmor radius in linear ITG stability study, the mode structure becomes localized with respect to k_{θ} and a structure similar to the one presented in Figure 7 is found, as has for instance been shown with a Multi Water Bag model [26,27].

It should finally be noted that a fundamental difference between ITG and ETG modes lies in the difference between the adiabatic electrons and respectively ions responses: the electrostatic potential experienced by the electrons has indeed to be corrected by its average on each flux surface of interest:

$$\delta n_{\mathrm{e,\ ad.}} \propto \phi - \langle \phi \rangle_{\mathrm{FS}},$$

while it is not the case for the adiabatic ion response:

$$\delta n_{\mathrm{i,\ ad.}} \propto \phi.$$

These different responses play a fundamental role in the non-linear physics of the ITG and ETG driven turbulence, by changing significantly the dynamics of Zonal Flow [6].

5 Discussion

The Multi Water Bag model has been adapted to kinetic electrons, for studying the linear stability of the drift kinetic equation in cylindrical geometry. The Multi Water Bag model offers an interesting connection between kinetic and hydrodynamic equations. Despite the model developed and the dielectric plasma function obtained are valid for a multi species case, including electrons and an arbitrary number of ions, we limit our analysis to pure electron temperature gradient modes.

The electron Larmor radius being approximately the same order as the Debye length in a tokamak, the usual assumption of quasi-neutrality is not appropriate. However, under the assumption of large radial and azimuthal extents of the linear modes, the Laplacian operator inherited from Poisson equation can be reduced to its poloidal component $\lambda_{De}^2 \triangle \phi \approx -\lambda_{De}^2 k_{\theta}^2 \phi$. The linear properties of the electron temperature gradient modes have been exhaustively analyzed.

Similarities between the ion temperature gradient and the electron temperature gradient modes are found, especially, the global structure of the linear stability threshold is observed almost identical. In the case of a flat density profile, the fluid limit estimate of the linear growth rate exhibits the same dependence on the logarithmic temperature gradient $\gamma \propto \kappa_{Te}^{1/3}$, and the fluid limit is shown to overestimate the linear growth rate by a factor 2. The ETG linear growth rate is shown to admit a maximum

along the parallel and poloidal wave vectors, recovering the tendency of ETG modes to develop a streamer structure. Taking into account polarization effect can be done simply by using an aternative choice of normalization for the poloidal wave vector k_θ as well as for the bag gradients κ_{sj}. Similarities are found with the mode structure of the linear ITG modes, with the important difference that finite Larmor radius effects play an impotant role for ITG. This similarity with previous observations has however to be taken with care, since our model is not including magnetic curvature and gradient drifts, and consequently does not allow to describe trapped electron modes (TEM) nor magnetic shearing effects, that are known to be important in the properties of the electron induced transport [18].

A next step consists in the study of the linear properties of kinetic ions and electrons in the same framework: the large values of the mass ratios will require special attention. The choice made in normalizing the equilibrium bag velocities $\pm a_{sj}$ to the associated thermal velocities v_{Ts} allows to manipulate comparable numbers, and will facilitate this enrichment. The linear stability properties of a plasma including kinetic ions and electrons is especially interesting when considering trapped particles.

Neglected in this paper, finite Larmor radius effects, as well as toroidal geometry are important steps for the future works, allowing for comparisons with existing gyrokinetic linear solvers, as well as with experiments.

The toroidal geometry is a key ingredient for including trapped particles (electrons as well as ions), that are known to play an important role in the linear properties of the plasma, for instance Trapped Electron Modes are known to develop streamers at scales close to the ion gyro radius. This overlap between ion and electron linear scales motivates also the extension of the model to a multi species one, allowing to study the linear properties of ion as well as electron scales. Moreover, the toroidal geometry introduces a radial dependence in the parallel wave number, so that toroidal mode coupling, as well as magnetic shear can affect strongly the linear properties of ETG modes and allow to reduce the electron transport [52]. It should finally be noted, regarding the geometry, that the magnetic shear effect can be already included in a cylindrical geometry, by considering a radial profile for the background magnetic field.

Neglecting finite Larmor radius effects has allowed to reduce significantly the complexity of the problem. Finite Larmor radius effects are however known to be important in introducing the polarization term in the Poisson equation and gyroaveraging operators in gyrokinetic Vlasov and Poisson equations (6)−(9). At second order, these FLR terms can be expressed as Laplacian operators restricted to the plane perpendicular to the magnetic field. Regarding our model, taking into account FLR effects consists then in adding new complicated terms under the Laplacian, but does not fundamentally changes the structure of the dielectric plasma function and the different assumptions made.

An adaptation of the existing quasi-linear and nonlinear Multi Water Bag codes [53,54] to the study of ETG induced turbulence is also a promising work under consideration. This should allow to access to a global description of micro-turbulence in a cylindrical plasma column, that can be of interest for comparisons with experiments, as well as in giving insights for reduced models of plasma micro-turbulence.

Authors would like to thank P. Bertrand and E. Gravier for helpful discussions.

References

1. X. Garbet, Y. Idomura, L. Villard, T.H. Watanabe, Nucl. Fusion **50**, 043002 (2010)
2. J.A. Krommes, Ann. Rev. Fluid Mech. **44**, 175 (2012)
3. P. Morel, E. Gravier, N. Besse, R. Klein, A. Ghizzo, P. Bertrand, W. Garbet, Ph. Ghendrih, V. Grandgirard, Y. Sarazin, Phys. Plasmas **14**, 112109 (2007)
4. T. Görler, F. Jenko, Phys. Rev. Lett. **100**, 185002 (2008)
5. Z. Lin, T.S. Hahm, W.W. Lee, W.M. Tang, R.B. White, Science **281**, 1835 (1998)
6. P.H. Diamond, S.-I. Itoh, K. Itoh, T.S. Hahm, Plasma Phys. Control. Fusion **47**, R35 (2005)
7. T. Estrada, T. Happel, C. Hidalgo, E. Ascasíbar, E. Blanco, Europhys. Lett. **92**, 35001 (2010)
8. V. Berionni, Ö.D. Gürcan, Phys. Plasmas **18**, 112301 (2011)
9. P. Morel, V. Berionni, Ö.D. Gürcan, Plasma Phys. Control. Fusion **56**, 015002 (2014)
10. W. Horton, B.G. Hong, W.M. Tang, Phys. Fluids **31**, 2971 (1988)
11. B.W. Stallard et al., Phys. Plasmas **6**, 1978 (1999)
12. W. Horton, P. Zhu, G.T. Hoang, T. Aniel, M. Ottaviani, X. Garbet, Phys. Plasmas **7**, 1494 (2000)
13. F. Jenko, W. Dorland, M. Kotschenreuther, B.N. Rogers, Phys. Plasmas **7**, 1904 (2000)
14. F. Jenko, W. Dorland, G.W. Hammett, Phys. Plasmas **8**, 4096 (2001)
15. F. Jenko, W. Dorland, Phys. Rev. Lett. **89**, 225001 (2002)
16. Ö.D. Gürcan, P.H. Diamond, Phys. Plasmas **11**, 572 (2004)
17. Ö.D. Gürcan, P.H. Diamond, Phys. Plasmas **11**, 4973 (2004)
18. Z. Lin, L. Chen, F. Zonca, Phys. Plasmas **12**, 056125 (2005)
19. W.M. Nevins, J. Candy, S. Cowley, T. Dannert, A. Dimits, W. Dorland, C. Estrada-Mila, G.W. Hammett, F. Jenko, M.J. Pueschel, D.E. Shumaker, Phys. Plasmas **13**, 122306 (2006)
20. A. Brizard, T.S. Hahm, Rev. Mod. Phys. **79**, 421 (2007)
21. D.C. DePackh, J. Electron. Control **13**, 417 (1962)
22. M.R. Feix, F. Hohl, L.D. Staton, in *Nonlinear Effects in Plasmas*, edited by G. Kalmann, M.R. Feix (Gordon and Breach, New York, 1969), pp. 3–21
23. P. Bertrand, M.R. Feix, Phys. Lett. A **28**, 68 (1968)
24. P. Bertrand, M.R. Feix, Phys. Lett. A **29**, 489 (1969)
25. H.L. Berk, K.V. Roberts, in *Methods in Computational Physics*, edited by B. Alder, S. Fernbach, M. Rotenberg (Academic Press, New York, 1970), Vol. 9, p. 29
26. N. Besse, P. Bertrand, P. Morel, E. Gravier, Phys. Rev. E **77**, 056410 (2008)

27. R. Klein, E. Gravier, J.H. Chatenet, N. Besse, P. Bertrand, X. Garbet, Eur. Phys. J. D **62**, 413 (2011)
28. E. Gravier, R. Klein, P. Morel, N. Besse, P. Bertrand, Phys. Plasmas **15**, 122103 (2008)
29. E. Gravier, E. Plaut, Phys. Plasmas **20**, 042105 (2013)
30. G.G. Howes, S.C. Cowley, W. Dorland, G.W. Hammett, E. Quataert, A.A. Schekochihin, Astrophys. J. **651**, 590 (2006)
31. U. Finzi, Plasma Phys. **14**, 327 (1972)
32. M.R. Feix, P. Bertrand, A. Ghizzo, in *Advances in Kinetic Theory and Computing*, Series on Advances in Mathematics and Applied Science, edited by B. Perthame (World Scientific, Singapore, 1994), Vol. 22, pp. 42–82
33. M. Navet, P. Bertrand, Phys. Lett. A **34**, 117 (1971)
34. P. Bertrand, Ph.D. thesis, Université de Nancy, France, 1972
35. P. Bertrand, J.P. Doremus, G. Baumann, M.R. Feix, Phys. Fluids **15**, 1275 (1972)
36. P. Bertrand, M. Gros, G. Baumann, Phys. Fluids **19**, 1183 (1976)
37. P.J. Catto, Plasma Phys. **20**, 719 (1978)
38. R.G. Littlejohn, J. Math. Phys. **23**, 742 (1982)
39. E.A. Frieman, L. Chen, Phys. Fluids **25**, 502 (1982)
40. D.H.E. Dubin, J.A. Krommes, C. Oberman, W.W. Lee, Phys. Fluids **26**, 3524 (1983)
41. W.W. Lee, Phys. Fluids **26**, 556 (1983)
42. T.S. Hahm, Phys. Fluids **31**, 2670 (1988)
43. T.S. Hahm, Phys. Plasmas **3**, 4658 (1996)
44. H. Sugama, Phys. Plasmas **7**, 466 (2000)
45. A.J. Brizard, Phys. Plasmas **7**, 4816 (2000)
46. A.A. Schekochihin, S.C. Cowley, W. Dorland, G.W. Hammett, G.G. Howes, G.G. Plunk, E. Quataert, T. Tatsuno, Plasma Phys. Control. Fusion **50**, 124024 (2008)
47. B. Scott, J. Smirnov, Phys. Plasmas **17**, 112302 (2010)
48. F.I. Parra, P.J. Catto, Phys. Plasmas **17**, 056106 (2010)
49. M. Gros, P. Bertrand, M.R. Feix, Plasma Phys. **20**, 1075 (1978)
50. P. Morel, E. Gravier, N. Besse, A. Ghizzo, P. Bertrand, Commun. Nonlinear Sci. Numer. Simul. **13**, 11 (2008)
51. Y. Sarazin, V. Grandgirard, G. Dif-Pradalier, X. Garbet, Ph. Ghendrih, Phys. Plasmas **13**, 092307 (2006)
52. J.L. Peterson, R. Bell, J. Candy, W. Guttenfelder, G.W. Hammett, S.M. Kaye, B. LeBlanc, D.R. Mikkelsen, D.R. Smith, H.Y. Yuh, Phys. Plasmas **19**, 056120 (2012)
53. D. Coulette, N. Besse, J. Comput. Phys. **248**, 1 (2013)
54. D. Coulette, N. Besse, Phys. Plasmas **20**, 052107 (2013)